Size effects in cellular solids

Tekoğlu, Cihan

1 Introduction

When modern man builds large load-bearing structures, he uses dense solids; steel, concrete, glass. When nature does the same, she generally uses cellular materials; wood, bone, coral. There must be good reasons for it.

M .F. Ashby

1.1 Cellular solids

Natural materials, such as wood, cork and cancellous bone, and man-made materials such as metal honeycombs and foams, are well-known examples of cellular solids. Common to all of them is a microstructure consisting of an interconnected network of struts (open cells) or plates (closed cells). Figure 1.1.a-c show three examples of cellular solids, namely, a hexagonal honeycomb, an open and a closed cell foam, respectively.

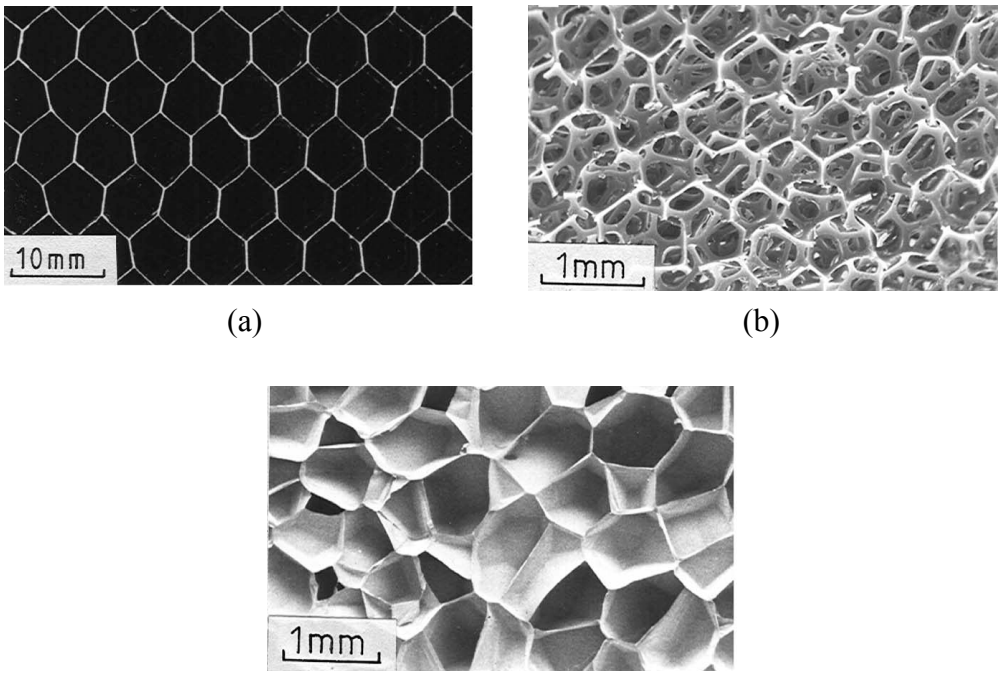

(a) (b)

(c)

Figure 1.1: Examples of cellular solids: (a) Aluminium honeycomb. (b) Open cell polyurethane foam. (c) Closed cell polyethylene foam. (Reproduced, with permission, from Gibson and Ashby [1997]).

Theoretical attempts to understand the geometry and the fundamental principles of the mechanics of cellular solids dates back to the celebrated geometrician Leonard Euler (see De Boor [1998]). Since then, a large literature developed on the geometric, mechanical, thermal and electrical characteristics of these solids. An extensive record on the structure and the properties of cellular solids is given by Gibson and Ashby [1997]. In this thesis, we focus on the mechanics of metal honeycombs and foams, yet, most of our conclusions are applicable to other cellular solids as well.

The high specific bending stiffness is an important structural property, which, among others, has made metal foams a competitive engineering material in the last decades. They are often used in sandwich panels, where they are laminated between two dense solids to increase the moment of inertia, owing to their low density and good shear and fracture strength. Their damping capacity is up to 10 times that of the solid metals, and they have exceptional ability to absorb energy at almost constant strain, which makes them attractive for impact absorption systems. Open cell foams, with a large accessible surface area, have a very good heat transfer ability. A more extensive list of multifunctional features and application areas for a number of commercially available metal foams are given by Ashby *et al*. [2000]. Metal foams have already a profitable market, which is growing rapidly due to the improvements in the production technology and engineering design.

1.2 Objective

The mechanical properties of metal foams (and other cellular solids) depend on the properties of the metal that they are made from, on their relative density, and on the cell topology (i.e., cell size, cell shape, open or closed cell morphology, etc.). The cell size of commercially available metal foams is about 1 to 10 mm. This is on the order of the smallest structural length of specimens in many applications. In such cases, the individual response to a load differs significantly from one cell to another, and the fundamental assumption of the classical continuum theory that the (physical, chemical, mechanical, etc.) properties of a material are uniformly distributed throughout its volume fails. Another situation where the classical continuum theory loses its accuracy is when the characteristic wavelength of loading is comparable to the cell size. An important technological consequence of this is the occurrence of size effects. The term "size effect" designates the effect of the macroscopic (sample) size, relative to the cell size, on the mechanical behaviour. In the last decade evidence of this appeared in a number of experimental studies (see section 1.4). To theoretically account for size effects, one may take the cellular morphology into account by discretely modelling each cell wall and/or cell face. This allows for an accurate representation of the microstructural deformation mechanisms, the bending and stretching of cell walls and faces. Such a microstructural model can predict how the overall (macroscopic) response is related to the microstructural parameters. In view of size effects, the most important feature is that it incorporates, in a physically sound manner, the material length scale in the problem, i.e. the cell size. However, such a discrete model can become computationally expensive for complex (random) microstructures, especially in three dimensions. Another approach is to use a generalized continuum theory in which many microstructural details are averaged out,

but in which a "characteristic" length scale is retained. The goal of this thesis is twofold:
1) To explore the microstructural mechanisms that are responsible for the size-dependent elastic behaviour of cellular solids by using a discrete microstructural model.
2) To assess the capability of generalized continuum theories to capture size effects through a careful comparison with the discrete simulations.

In section 1.3, we give a historical overview of generalized continuum theories. We discuss two of them in more detail, Eringen's micropolar theory and Toupin-Mindlin's strain gradient elasticity. In section 1.4, we summarize the experimental work performed to detect the size effects in the mechanics of cellular solids. Finally, in section 1.5, we outline the contents of this thesis.

1.3 Generalized continuum theories: a historical overview

A natural generalization of the classical continuum theory is to model the interaction between two material points, not only via a force vector, but also via a couple vector. The origin of this evolution can be traced back to the early Euler-Bernoulli beam theory, where the displacement and the rotation vectors are independent kinematic quantities, and the usual force tractions and couples are independent internal loads. The idea of having independent couple-stresses in an elastic continuum is further explored by several scientists in the 18'th century (MacCullagh (1839), Lord Kelvin (1882, 1884, 1890), Voigt (1887))[1]. In 1909, E. and F. Cosserat (the Cosserat brothers) developed a (non-linear) theory of elasticity for bars, surfaces and bodies; they introduced a "rigid triad" at every material point of the continuum, which can rotate independently from the local rotation of the medium in the course of deformation (Cosserat and Cosserat [1909]). By this way, a "Cosserat continuum" fully accounts for the effects of couple stresses in the deformation of an elastic continuum. In their work, however, the Cosserat brothers did not give any specific constitutive relations.

The work of the Cosserat brothers did not get the attention it deserved for a long time. In the early 1960s, the subject of the theory of elasticity with couple stresses is reopened and Cosserat-type theories are discussed independently by several authors. Among them, Grioli [1960], Rajagopal [1960], Truesdell and Toupin [1960], Aero and Kuvshinskii [1961], Eringen [1962], Mindlin and Tiersten [1962] and Koiter [1964] investigated a special case of the Cosserat continuum theory where the rotation of the rigid Cosserat triad is not an independent kinematic variable but is defined in the usual sense as given in classical elasticity and fluid dynamics. In the

[1] See Cosserat and Cosserat [1909] and the references therein.

literature, this theory is referred to with a variety of names, such as, "Cosserat theory with constrained rotation" (e.g. Toupin [1964]), "Couple stress theory" (e.g. Koiter [1964]), "Indeterminate couple stress theory" (e.g. Eringen [1968]), "Cosserat pseudo-continuum" (e.g. Nowacki [1986]), or simply as "Cosserat theory" (e.g. Mora and Waas [2000]). In the following, we will refer to it as the couple stress theory (see Table 1.1). In the couple stress theory, only the gradient of the rotation vector enters into the strain energy density function, that is, eight of the eighteen components of the first gradient of strain. Subsequently, all the components of the first gradient of the strain were introduced into the strain energy density function, in a non-linear form, by Toupin [1962, 1964]). This theory is referred to as the "strain gradient theory" in the literature. The linear version of the strain gradient theory was given by Mindlin [1964]. Green and Rivlin [1964] established the basis of a very general case including all higher-order gradients of the strain, referred to as the "multipolar" theory. Mindlin [1965] derived a theory where both the first and the second gradient of the strain are taken into account, termed the second strain gradient theory, which is a special case of the multipolar theory. All these theories, associating energy to the spatial gradients of strain, are referred to in the literature as "higher grade theories" (see Table 1.1).

Another way of extending classical elasticity to include the effects of the deformations of the underlying microstructure is by inserting new degrees of freedom into the continuum. These degrees of freedom are specified to be independent from the usual displacement degrees of freedom. These kinds of theories can be referred to as "higher order theories" (see Table 1.1). The (non-linear) micromorphic theory, introduced by Eringen and Şuhubi [1964], and the (linear) micro-structure theory of Mindlin [1964] fall into this category. The linear form of the micromorphic theory (see Eringen [1999]) coincides with the micro-structure theory of Mindlin. In the micromorphic theory, a material point possesses three deformable directors that introduce nine additional degrees of freedom, ψ_{ij}, which are strain-like dimensionless quantities. This corresponds to a "micro-element" embedded in the continuum that can rotate and deform independently from the local deformation of the "macro-element" (material particle), in the language of Mindlin. Two special cases of the micromorphic theory are the microstretch (Eringen [1971, 1990]) and the micropolar (Eringen [1965, 1966]) theories. In the microstretch continuum, there are four additional degrees of freedom: three for the rotation (ϕ_i) and one for the stretch (χ) of the directors. In the case of the micropolar continuum, the directors are rigid and there are only three rotational degrees of freedom (ϕ_i) in addition to the three classical displacement degrees of freedom. If the directors are taken to be fully coupled to the material point, the rotational degrees of freedom of the micropolar theory become equal to the classical rotations, $\phi_k = \in_{ijk} u_{j,i}/2$, and the micropolar theory reduces to the couple stress theory. As can be observed from Table 1.1, the couple stress theory is a special case of strain gradient theory as well. Another connection between the

higher order and higher grade theories is that the micromorphic theory reduces to the strain gradient theory if ψ_{ij} are defined to be equal to the gradient of displacement $u_{i,j}$, for which case the micro-medium merges with the macro-medium.

In the last few decades, a huge literature has been built up on the topic of generalized media, including elasto-plastic higher order/grade continuum theories (see e.g., Aifantis [1987], Fleck and Hutchinson [1993, 1997, 2001], Forest and Sievert [2006], etc.). The references listed here are by no means complete, but they point out the main directions followed in the field of generalized continuum theories. Table 1.1 summarizes (some of) the higher order/grade continuum theories and the contacts among them. Starting point for the higher order and the higher grade theories in this thesis are Eringen's micropolar theory and Toupin-Mindlin's strain gradient elasticity. Therefore, we will briefly state the fundamentals of these theories in the following subsections.

1.3.1 Theory of micropolar elasticity

In this section we will review the fundamental equations of the linear micropolar continuum. For a more general account of the theory, the reader is referred to Eringen [1999]. Note that the names micropolar theory and Cosserat theory are used interchangeably by many authors in the literature.

The kinematic description of the micropolar theory includes the microrotations ϕ_i as independent degrees of freedom in addition to the usual displacements u_i (see Table 1.1). Consequently, the transfer of loading between neighbouring material points is achieved both through the couple stresses m_{ij} and the classical Cauchy stresses σ_{ij}. In the absence of body forces and body couples, the equilibrium equations of the micropolar theory are given as

$$\begin{aligned} &\sigma_{ji,j} = 0, \\ &m_{ji,j} + \in_{ijk} \sigma_{jk} = 0, \end{aligned} \tag{1.1}$$

where $\in_{ijk}$ is the antisymmetric Levi-Civita permutation tensor. Equation (1.1) implies that the Cauchy stress tensor σ_{ij} is not necessarily symmetric and its antisymmetric part is determined by the divergence of the couple stress tensor m_{ij}. The principal of virtual work reads

$$\int_V (\sigma_{ij}\delta\gamma_{ij} + m_{ij}\delta k_{ij})\, \mathrm{d}V = \int_S (t_i \delta u_i + Q_i \delta\phi_i)\, \mathrm{d}S, \tag{1.2}$$

where t_i is the surface traction, and Q_i is the surface couple. The boundary conditions to be specified on the bounding surface S of a micropolar solid are

Table 1.1

Higher order/grade continuum theories and the contacts among them.

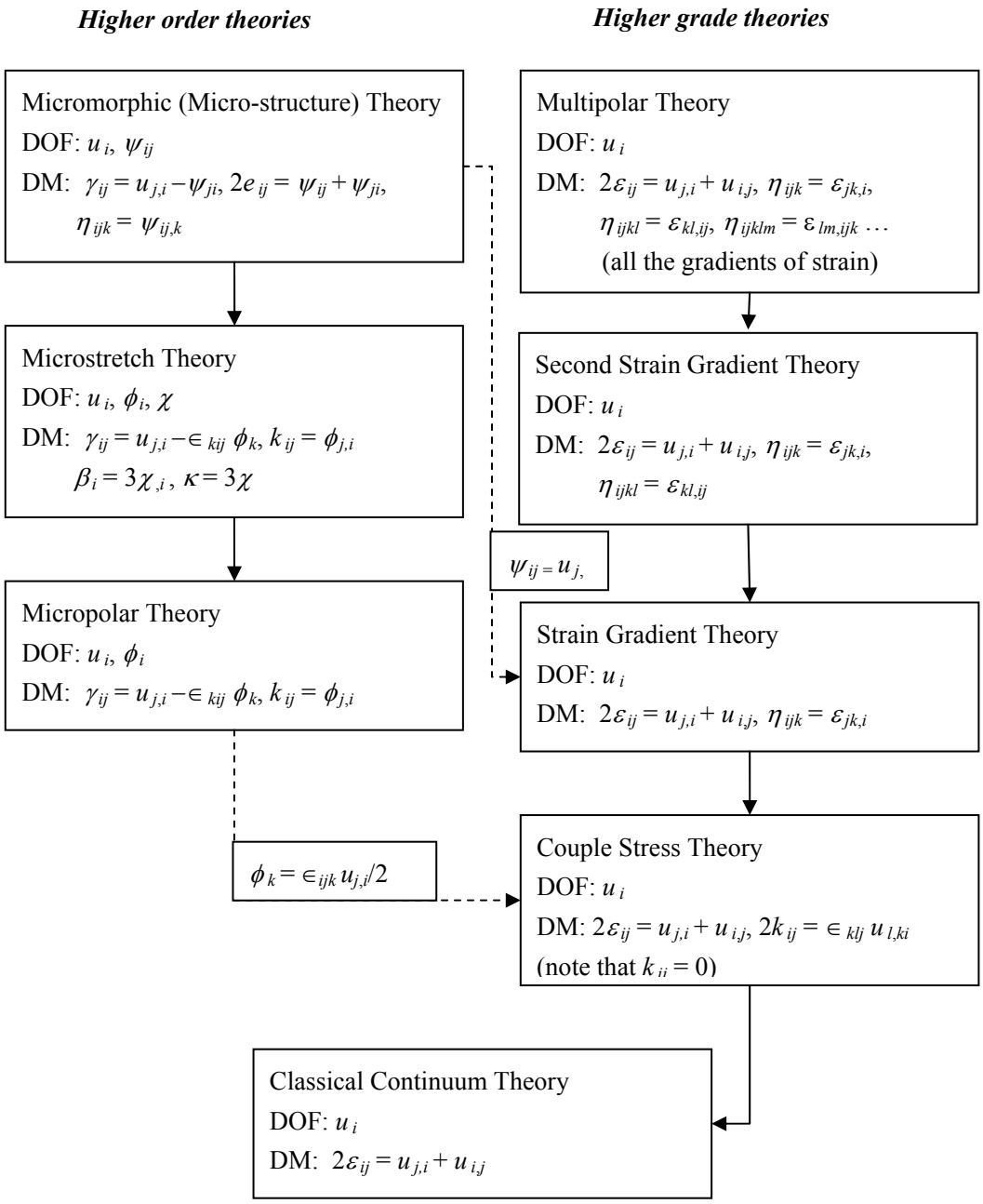

DOF: degree of freedom, DM: deformation measure,

ψ_{ij}: degree of freedom tensor for the deformable triad (micro-element),

u_i: displacement vector, ϕ_i: rotation vector for the rigid triad

$$\begin{aligned} n_j \sigma_{ji} &= t_i^* \quad \text{or} \quad u_i = u_i^*, \\ n_j m_{ji} &= Q_i^* \quad \text{or} \quad \phi_i = \phi_i^*, \end{aligned} \tag{1.3}$$

where n_j is the unit outward normal to the surface S, and * denotes a prescribed quantity on the surface. The (small) strain tensor γ_{ij} and the curvature tensor k_{ij} are defined as

$$\begin{aligned} \gamma_{ij} &= u_{j,i} - \in_{kij} \phi_k, \\ k_{ij} &= \phi_{j,i}. \end{aligned} \tag{1.4}$$

We can decompose the Cauchy stresses and strains into their symmetric and antisymmetric parts

$$\sigma_{ij} = s_{ij} + \tau_{ij} \text{ and } \gamma_{ij} = \varepsilon_{ij} + \beta_{ij}, \tag{1.5}$$

where

$$\varepsilon_{ij} = \frac{1}{2}(\gamma_{ij} + \gamma_{ji}) = \frac{1}{2}(u_{j,i} + u_{i,j}) \text{ and } \beta_{ij} = \frac{1}{2}(\gamma_{ij} - \gamma_{ji}) = \in_{ijk} (\omega_k - \phi_k). \tag{1.6}$$

Note that the antisymmetric part of the strain β_{ij} is related to the difference between the classical macrorotations $\omega_k = (\in_{ijk} u_{j,i})/2$ and the microrotations ϕ_k.

For a linear elastic, anisotropic micropolar solid, a strain energy density function (i.e. including only the quadratic terms in the kinematic variables) can be given as

$$w(\gamma_{ij}, k_{ij}) = \frac{1}{2} C_{ijkl} \gamma_{ij} \gamma_{kl} + B_{ijkl} \gamma_{ij} k_{kl} + \frac{1}{2} D_{ijkl} k_{ij} k_{kl}. \tag{1.7}$$

In (1.7) the linear terms in γ_{ij} and k_{ij} are omitted to have zero stress in the undeformed state. Note that k_{ij} is a pseudo-tensor (i.e., a tensor whose components reverse sign under an inversion of the coordinate system); to be able to have an objective strain energy density w, the tensor B_{ijkl} must be a pseudo-tensor as well. The independence of the stiffness coefficients of a medium with respect to an inversion of the coordinate system is called *central symmetry*, in which case B_{ijkl} vanish and the constitutive equations read

$$\sigma_{ij} = \frac{\partial w}{\partial \gamma_{ij}} = C_{ijkl}\gamma_{kl},$$
$$m_{ij} = \frac{\partial w}{\partial k_{ij}} = D_{ijkl}k_{kl}, \tag{1.8}$$

where the fourth order stiffness tensors C_{ijkl} and D_{ijkl} possess the symmetries

$$C_{ijkl} = C_{klij} \quad \text{and} \quad D_{ijkl} = D_{klij}. \tag{1.9}$$

For the case of an isotropic material, C_{ijkl} and D_{ijkl} are isotropic tensors, and the constitutive equations read (see e.g. Nowacki [1986])

$$\begin{aligned} \sigma_{ij} &= \frac{\partial w}{\partial \gamma_{ij}} = (\mu+\alpha)\gamma_{ij} + (\mu-\alpha)\gamma_{ji} + \lambda\gamma_{kk}\delta_{ij}, \\ m_{ij} &= \frac{\partial w}{\partial k_{ij}} = (\xi+\upsilon)k_{ij} + (\xi-\upsilon)k_{ji} + \rho k_{kk}\delta_{ij}, \end{aligned} \tag{1.10}$$

where δ_{ij} is the Kronecker-delta. Equation (1.10) shows that the micropolar theory has four new constants, α, ξ, υ, and ρ in addition to the classical Lamé constants, λ and μ. The requirement of positive definiteness of the strain energy density places some restrictions on the micropolar constants:

$$\begin{aligned} &\mu > 0, \quad 3\lambda + 2\mu > 0, \quad \xi > 0, \quad 3\rho + 2\xi > 0, \\ &\mu + \alpha > 0, \quad \xi + \upsilon > 0, \quad \alpha > 0, \quad \upsilon > 0. \end{aligned} \tag{1.11}$$

If the microrotations ϕ_i are constrained to be equal to the macrorotations ω_i, the micropolar theory reduces to the couple stress theory. This corresponds to the case $\alpha \to \infty$, for which the antisymmetric part of the strain tensor, β_{ij}, and the spherical part of the curvature tensor, k_{ii}, go to zero. Consequently, the antisymmetric part of the Cauchy stress, τ_{ij}, and the first invariant of the couple stress, m_{kk}, disappear from the virtual work principle, as well as from the constitutive equations:

$$\begin{aligned} s_{ij} &= \lambda\varepsilon_{kk}\delta_{ij} + 2\mu\varepsilon_{ij}, \\ m_{ij} &= (\xi+\upsilon)k_{ij} + (\xi-\upsilon)k_{ji}. \end{aligned} \tag{1.12}$$

The first invariant of the couple stress, m_{kk}, remains indeterminate in the theory, and it is taken to be equal to zero (see Koiter [1964]). The antisymmetric part of the Cauchy

stress, τ_{ij}, can still be obtained from the equilibrium equations (see Eq. 1.1). For a discussion of the couple stress theory, the reader is referred to Koiter [1964].

1.3.2 Strain gradient elasticity

In this section we will review the fundamental equations of the strain gradient elasticity. For a more general account of the theory, the reader is referred to Mindlin [1964].

The kinematic variables in the strain gradient elasticity theory are given as

$$\begin{aligned} \varepsilon_{ij} &= \frac{1}{2}(u_{j,i} + u_{i,j}) = \text{strain tensor}, \\ \eta_{ijk} &= \varepsilon_{jk,i} = \eta_{ikj} = \text{strain gradient tensor}. \end{aligned} \tag{1.13}$$

The strain energy density function, for a linear elastic, isotropic strain gradient material with central symmetry can be written as

$$\begin{aligned} w(\varepsilon_{ij}, \eta_{ijk}) = \frac{\lambda}{2}\varepsilon_{ii}\varepsilon_{jj} + \mu\varepsilon_{ij}\varepsilon_{ij} + a_1\eta_{iik}\eta_{kjj} + a_2\eta_{ijj}\eta_{ikk} \\ + a_3\eta_{iik}\eta_{jjk} + a_4\eta_{ijk}\eta_{ijk} + a_5\eta_{ijk}\eta_{kji}. \end{aligned} \tag{1.14}$$

Note that the eighteen additional kinematic variables in the strain energy density function, η_{ijk}, can be defined in three different forms: I, the eighteen components of the second gradient of displacement; II, the eighteen components of the first gradient of strain; III, the eight components of the first gradient of the rotation and the ten components of the fully symmetric part of the second gradient of the displacement (or of the gradient of the strain) as shown by Mindlin [1964]. The one that we show here corresponds to the second form.

The constitutive equations (for the second form) are given as

$$\begin{aligned} \sigma_{ij} &= \frac{\partial w}{\partial \varepsilon_{ij}} = \lambda\varepsilon_{kk}\delta_{ij} + 2\mu\varepsilon_{ij}, \\ \tau_{ijk} &= \frac{\partial w}{\partial \eta_{ijk}} = \frac{1}{2}a_1(\delta_{ij}\eta_{kpp} + 2\delta_{jk}\eta_{ppi} + \delta_{ki}\eta_{jpp}) + 2a_2\delta_{jk}\eta_{ipp} \\ &\quad + a_3(\delta_{ij}\eta_{ppk} + \delta_{ik}\eta_{ppj}) + 2a_4\eta_{ijk} + a_5(\eta_{kij} + \eta_{jki}). \end{aligned} \tag{1.15}$$

In (1.15) the constants a_1 to a_5 are new material parameters with dimensions of force, σ_{ij} are the classical Cauchy stresses and τ_{ijk} are the so-called double stresses, with dimensions force per unit length. The positive definiteness of the strain energy density requires (see Mindlin and Eshel [1968])

$$\begin{aligned} &\mu > 0, \quad 3\lambda + 2\mu > 0, \quad -\bar{d}_1 < \bar{d}_2 < \bar{d}_1, \quad \bar{a}_2 > 0, \\ &5\bar{a}_1 + 2\bar{a}_2 > 0, \quad 5\bar{f}^2 < 6(\bar{d}_1 - \bar{d}_2)(5\bar{a}_1 + 2\bar{a}_2), \end{aligned} \tag{1.16}$$

where

$$\begin{aligned} &18\bar{d}_1 = -2a_1 + 4a_2 + a_3 + 6a_4 - 3a_5, \\ &18\bar{d}_2 = 2a_1 - 4a_2 - a_3, \quad 3\bar{a}_1 = 2(a_1 + a_2 + a_3), \\ &\bar{a}_2 = a_4 + a_5, \quad 3\bar{f} = a_1 + 4a_2 - 2a_3. \end{aligned} \tag{1.17}$$

The principal of virtual work for a volume V bounded by a smooth surface S, in the absence of body forces, reads

$$\int_V (\sigma_{ij}\delta\varepsilon_{ij} + \tau_{ijk}\delta\eta_{ijk})\, \mathrm{d}V = \int_S (t_j \delta u_j + r_j \delta D u_j)\, d\mathrm{S}, \tag{1.18}$$

where t_j and r_j are the surface traction and the surface double traction, respectively, on the surface S. The equilibrium equations and the boundary conditions are

$$\sigma_{jk,j} - \tau_{ijk,ij} = 0, \tag{1.19}$$

and

$$\begin{aligned} &n_j(\sigma_{jk} - \tau_{ijk,i}) - D_j(n_i\tau_{ijk}) + (D_l n_l) n_i n_j \tau_{ijk} = t_k^* \ \text{ or } \ u_k = u_k^*, \\ &n_i n_j \tau_{ijk} = r_k^* \ \text{ or } \ Du_k = Du_k^*, \end{aligned} \tag{1.20}$$

where n_j is the unit outward normal to the surface S. For a certain combination of the higher grade material constants, the strain gradient theory reduces to the couple stress theory:

$$\begin{aligned} &a_1 \to \xi - \upsilon, \quad a_2 \to -\frac{\xi - \upsilon}{2}, \quad a_3 \to -\frac{\xi - \upsilon}{2}, \\ &a_4 \to \xi, \quad a_5 \to -\xi. \end{aligned} \tag{1.21}$$

1.4 A brief summary of experiments on size effects

A considerable amount of experiments have been performed to capture the size effects in the mechanical behaviour of cellular solids. In this section, we will visit some of

these studies, which establish the experimental basis and an important motivation for this thesis.

The first experiments associated with size effects, to the knowledge of the author, were performed in the mid 1960s to obtain the couple stress constants of conventional engineering dense solids, such as aluminium and steel. Schijve [1966] measured the bending rigidity of aluminium sheets, but could not observe any size effects, as opposed to the couple stress theory which predicts an enhanced bending rigidity with decreasing plate thickness. Similarly, Ellis and Smith [1967] conducted bending tests on aluminium and low-carbon steel sheets, and they did not reveal any couple stress effects. They concluded that couple stress effects would be active only for much smaller sample sizes, where the plate thickness is approximately equal to the grain size. Then, experiments on micro-featured materials (such as reinforced composites) were conducted, which are expected to show higher-order effects for larger samples due to the larger microstructural length scales. Gauthier and Jahsman [1975] developed a novel composite material to measure its micropolar elastic constants. The composite consisted of an epoxy matrix reinforced by uniformly distributed aluminium shots, with a Young's modulus 20 times that of the matrix. The much stiffer aluminium shots represented rigid microelements embedded in a deformable medium (i.e. the epoxy matrix). They performed torsion tests on circular cylindrical samples, but the samples behaved according to the classical theory. They concluded: "Possible micropolar behaviour is masked by material property variations (from one sample to another with a different size) due to inhomogeneity". Gauthier [1982], however, was able to fit the wave propagation experiments on the same reinforced composite by using micropolar theory, with a characteristic length very close to the radius of the aluminium shots, 0.7 mm. Lakes and co-authors performed several experiments on different micro-featured solids, such as human bones. Yang and Lakes [1981], conducted quasi-static torsion tests on circular cylindrical compact bones, and showed that the couple stress theory can capture the enhancement in torsional rigidity with decreasing sample radius. They found the couple stress characteristic length to be around 0.15-0.25 mm, which is comparable to the diameter of the major structural element in compact bones, the osteon.

The early experiments on cellular solids to observe the dependence of the macroscopic material properties on the specimen size dates back to the 1980's. Lakes [1983, 1986] measured the bending and torsional rigidities of two polymeric foams and a syntactic foam, as a function of diameter. He concluded that the micropolar elasticity is a suitable model to pick-up the enhanced bending and torsional rigidities with decreasing diameter of the polymeric foams, whereas the syntactic foam behaves as a classical solid. Opposed to these results, however, some others indicated a decreasing bending and torsional stiffness/strength with decreasing sample size. For example, Brezny and Green [1990] measured the Young's modulus and the bending

strength (by three-point bending experiments) of a reticulated vitreous carbon foam consisting of relatively isotropic open cells, and found that both the modulus and the strength of this material decrease dramatically with decreasing specimen size. The weakening effects in both bending and torsion were detected for closed cell polymethacrylimide foam and open cell copper foam as well (Anderson *et al*. [1994], Anderson and Lakes [1994]).

Size effects in foams under uniaxial compression are also experimentally investigated. Bastawros *et al*. [1999] measured the Young's modulus and the compressive strength of closed cell Alporas aluminium foam, by changing the area under compression while keeping the length of the samples in the compression direction constant. Andrews *et al*. [2001], on the other hand, conducted uniaxial compression tests on square prisms of both closed cell Alporas and open cell Duocel foams, where the samples had identical geometry but different absolute size. Both sets of experiments, similar to the observations of Brezny and Green, showed that the Young's modulus and the compressive strength of the samples decrease dramatically with decreasing specimen size. The common conclusion to all of these studies showing a weakening in the (bending, torsional or compressive) stiffness and strength was that these size effects are actually "edge effects". The edge effects were related to an incomplete cell layer located at the surface of the specimens, which is included in the total specimen volume but contribute very little to the mechanical properties. Surface damage introduced by cutting or machining of specimens enhances these edge effects. Anderson and Lakes [1994] argued that the edge effects and the micropolar effects are usually both present and it is possible to observe weakening or strengthening behaviour depending on which one is more dominant.

Shear experiments on metal foams were also reported. These studies indicated an enhanced shear strength with decreasing sample thickness (e.g. Andrews *et al*. [2001], Chen *et al*. [2002]). In these experiments, the shear load is applied through face sheets that are perfectly bonded to the metal foam. As a result, the surface cells that are perfectly bonded to the top and the bottom face sheets are much more constrained compared to those located in the bulk. This gives rise to a gradient in deformation, so that "strong" boundary layers are formed adjacent to the face sheets; the volume fraction of these boundary layers increase with decreasing thickness and it leads to a higher shear strength. Kesler and Gibson [2002], conducted three point bending experiments on sandwich panels with an Alporas foam core, of varying size, with the panels designed to fail by core shear. By accounting for the size effects in the foam core shear strength, they were able to give a good estimate of the failure load of the panels.

Stress/strain concentrations due to notches, holes and inclusions in cellular solids are other topics of essential interest for experimental investigation. The effect of the notch size (relative to the cell size), is examined on aluminium closed cell

foams (Antoniou *et al*. [2004]). They observed that under uniaxial compression, the net section strength of double-edge-notched specimens is larger when the net section width is smaller, whereas it is insensitive to the net section width in the case of single-edge-notched specimens. Mora and Waas [2000] performed uniaxial compression tests on a plate of polycarbonate honeycomb with circular cells, containing a cylindrical hole and a rigid inclusion, respectively. They could not detect any size effects in the case of the hole, but were able to fit the strain fields near the circular inclusion with the couple stress theory, for a variety of inclusion sizes.

1.5 Outline of this thesis

The aim of this thesis is to explore the microstructural origin of the size effects in the mechanical behaviour of cellular solids, in particular of metallic foams, and to investigate/propose generalized continuum theories that can capture these size effects.

In chapter 2, we use two-dimensional beam networks to mimic real (three-dimensional) foams, which allow us to account for the discreteness of their microstructure. We perform simple shear, uniaxial compression, and pure bending tests on a large variety of samples, and calculate the change in the macroscopic mechanical properties corresponding to a change in size. We close the chapter with a summary of the size effects that we observed in our calculations and discuss the possible mechanisms behind these size effects.

Chapter 3 uses the micropolar theory to capture the size effects observed in chapter 2. We fit the elastic constants of the micropolar continuum theory by comparing the analytical solution of the simple shear problem with the discrete analyses, in terms of the best agreement in the macroscopic shear stiffness of the samples. We develop a strain mapping procedure and evaluate the performance of the fitted micropolar constants in predicting the local deformation fields, the microrotations and shear strains. Finally, we solve the pure bending problem analytically for the micropolar theory and close the chapter with a discussion on the limitations of the Cosserat-type theories.

In chapter 4, we propose a generalized continuum theory (strain divergence theory), which associates energy to the divergence of strain. We derive the equilibrium equations and the boundary conditions for the strain divergence continuum, and develop a finite element implementation of the theory. We solve the simple shear and the pure bending problems analytically and compare the solutions with the discrete calculations, as well as with the analytical solutions for the couple stress theory.

Chapter 5 explores the strain concentration problem around a cylindrical hole in a field of uniaxial tension. First, we perform discrete calculations on samples with different hole sizes and show the effect of the hole size on the strain distribution near

the hole. Then we compare the discrete analyses with the analytical solutions for the classical, couple stress and strain divergence theories.

Finally, in Chapter 6, we summarize the size effects that we observed in the mechanical behaviour of the two dimensional cellular solids, and we compare the different generalized continuum theories with respect to their ability in capturing size effects.